Preprints of the 21st IFAC World Congress (Virtual)
Berlin, Germany, July 12-17, 2020

Monitoring the Moisture Content in Pharmaceutical Batch Fluidized Bed Dryers Using Observer-Based Soft Sensors

Marc-Olivier Roseberry * **Francis Gagnon** * **André Desbiens** *
Jocelyn Bouchard ** **Pierre-Philippe Lapointe-Garant** ***

* *Department of Electrical and Computer Engineering, LOOP, Université Laval, Québec City, Québec, G1V 6A6, Canada*
** *Department of Chemical Engineering, LOOP, Université Laval, Québec City, Québec, G1V 6A6, Canada*
*** *Process Monitoring Automation and Control, Global Engineering, Pfizer, Montréal, Québec, H4R 1J6, Canada*

Abstract: Tablet manufacturing in the pharmaceutical industry involves batch fluidized bed drying for particle moisture removal. This paper introduces five approaches for moisture content monitoring, relying either on a complex phenomenological model or its simplified version. The first two soft sensors consist of open-loop estimators, i.e. they simply simulate the models fed by the manipulated variables. Three closed-loop moving horizon estimators based on the simplified model are also proposed for improved robustness. In the first one, the measurements of the inlet gas and particle temperatures feed back the soft sensor. The last two closed-loop observers additionally can take into account infrequent delayed moisture content measurements, such as at-line loss on drying analysis. A validation of the soft sensors is performed with experimental data collected on a pilot scale fluidized bed dryer. Results show that the closed-loop observer with the delayed moisture content measurements still has an accuracy that is equivalent (and sometimes better) than the complex phenomenological model.

Keywords: state estimation, batch fluidized bed dryer, moving horizon estimator, offline measurement, measurement delay

1. INTRODUCTION

Fluidized bed dryers (FBD) are commonly used in pharmaceutical and food industries to remove excess of solvent or water in solid materials, such as powders, by injecting a continuous flow of a heated gas to force mass transfer. The main objective in pharmaceutical batch drying is to reach the desired moisture content without exceeding a given constraint, such as a maximum particle temperature. Model predictive control has shown to be an efficient technique for reducing cycle time (Obrégon et al., 2013) and energy consumption (Gagnon et al., 2017), using in this case a state estimator with moisture content measurement feedback provided by a near-infrared (NIR) spectrometer.

NIR spectroscopy is a fast and non-destructive analytical technique, widely used in pharmaceutical and food industry for monitoring the moisture content (Roggo et al., 2007). However, in the case of the FBD, NIR moisture measurement is only reliable if the probe window is cleared of powder accumulation and if particle fluidization is established sufficiently (Tok et al., 2008). Moreover, NIR spectroscope requires calibration that can hardly be transferred between pharmaceutical products, devices and equipment (Roggo et al., 2007).

Moisture content soft sensors could present alternatives or back-up solutions to the NIR probe. For instance, Jensen et al. (2011) proposed applications developed using empirical models, Vieira et al. (2019) using machine learning method such as artificial neural networks, and Zhang et al. (2019), using Random Forest to monitor drying processes. Lauri Pla et al. (2018) also proposed an estimator based on mass and energy balance for pharmaceutical FBD. Although these approaches could accurately estimate moisture content, they cannot predict the behavior of the system, and thus they can hardly be applied in a predictive control context. Process disturbances, differences in pharmaceutical compounds and equipment size can also be an issue when transferring this kind of soft sensor between products or between different manufacturing lines/equipment. Re-calibration is required in such case, which is known to be time consuming. Moreover, the main weakness of open-loop approaches is the potential process evolution/variance over extended periods of time that may cause the model to lack fit or accuracy over time. Use of such models thus would require a periodic model check and/or periodic model maintenance. For these reasons, industrial applications must integrate measurement feedback and filtering properties of a nonlinear state estimator like an extended Kalman filter (Li and Duncan, 2008) or moving horizon estimator (Gagnon et al., 2017).

A moving horizon estimator (MHE) is a fixed-size window optimization-based observer described by Rao and Rawlings (2002) that takes into account the last N mea-

surement to estimate the model states. Compared to the extended Kalman filter, the MHE main advantages are that it can handle nonlinear dynamics (without linearization) and state constraints (Haseltine and Rawlings, 2005). Moreover, the MHE observation window offers a simple way to handle measurements provided with variable delays (Valencia et al., 2011).

This work presents different approaches for moisture content monitoring. They rely either on a complex phenomenological model (two-phase) or its simplified version (single phase). The same manipulated variables, i.e. the air inlet temperature and volumetric flow rate controller setpoints, feed both these models. The first two soft sensors are open-loop estimators, i.e. they simply compute the deterministic predictions based on these models. Three closed-loop MHE soft sensors based on the simplified model are also described. Only the inlet gas and particle temperature measurements feed back the first one, but the second one also relies on sporadic delayed moisture content measurements, and the third one, on additional propagation of them to generate a sequence of virtual measurements. Estimated errors with experimental data collected on a pilot scale FBD allow validating the performance of all five soft sensors.

This paper is organized as follows. Section 2 summarizes the experimental setup. The two-phase and single phase models are presented in Section 3, and Section 4 describes the five observers. Section 5 highlights, and discusses the main results.

2. MATERIALS

Two-phase and single phase FBD models were calibrated with experimental data collected on a 1 ft^3 pilot scale FBD. The experimental setup is the same as the one described in Gagnon et al. (2020a). An Aeromatic MP-1 fluidized bed dryer is used to dry 3.14 kg calcium carbonate powder granulated with two excipients in small quantity. 0.712 kg of purified water is also incorporated. Inlet gas and particle temperature are measured with resistance temperature detectors (RTD).

Two independent methods provide moisture content measurements during the FBD operation: (1) a reliable inline moisture content given by a Viavi Solutions MicroNIR^{TM} Pro near-infrared (NIR) spectrometer paired with a pre-calibrated partial least squares model, and (2) an offline sample differential mass analysis.

3. BATCH FLUIDIZED BED DRYER MODELS

Gagnon et al. (2020a) proposed a two-phase FBD state-space model based on the Kunii-Levenspiel theory for pharmaceutical applications. The two-phase model was calibrated by a grey-box approach with experimental datasets collected on the pilot FBD. Simulation of the two-phase model was able to reproduce the pilot data accurately with moderate computational effort. However, when implemented in optimization-based estimation or control algorithms, solving the model represents an excessive computational burden.

A simpler model is required to design the closed-loop observers. Thus, Gagnon et al. (2020b) describe a single phase FBD model, in which major simplifications to heat and mass transfer are proposed. The single phase model describes the continuous state-space representation from which the closed-loop observer are designed. The following paragraphs succinctly describe the single phase dryer model equations and main assumptions.

Compared to the two-phase model, bubble phase is neglected. Thus, the FBD content is considered to be a single emulsion phase fluid composed of wet solid particles and interstitial gas at a constant void fraction. The total mass of particles m_p in the FBD is :

$$m_p = m_s + m_w \tag{1}$$

where m_s is the mass of solid material contained in the FBD vessel. Thus, m_w is the total mass of liquid water including free and bound moisture. The particle moisture content in dry basis is:

$$\chi_p = \frac{m_w}{m_s} \tag{2}$$

The mass balance is expressed in dry basis, but moisture content measurement is given by the NIR probe in wet basis. The particle moisture content in wet basis is evaluated by :

$$w_p = \frac{m_w}{m_w + m_s} = \frac{\chi_p}{1 + \chi_p} \tag{3}$$

The moisture content in dry basis can be evaluated by the following equation which will come handy to implement offline moisture content measurement :

$$\chi_p = \frac{w_p}{100 - w_p} \tag{4}$$

The moisture content gradient is the driving force of the evaporation process. For simplicity purposes, an exponential empirical function describes the saturation mixing ratio :

$$\gamma(T_p) = \alpha \exp(\beta T_p) \tag{5}$$

where T_p is the particle temperature. α and β are empirical coefficients.

Solid moisture removal kinetics are usually divided in two parts for non-hygroscopic material. Prior to the critical moisture content χ_{pc}, the drying rate is considered constant at isothermal conditions (constant rate period). Past this point, the drying rate starts to decrease (falling rate period). Since the moisture needs to diffuse from the particle internal pores to the surface to evaporate, the moisture content gradient should be limited in the falling rate period, hence the empirical function :

$$\psi(\chi_p) = \begin{cases} 1 & \text{if } \chi_p \geq \chi_{pc} \\ (\frac{\chi_p}{\chi_{pc}})^{\nu} & \text{if } \chi_p < \chi_{pc} \end{cases} \tag{6}$$

where ν is an empirical coefficient describing the drying rates.

3.1 Mass balance

During drying, the gradient between the inlet gas moisture content χ_0 and particle film drives the water removal from the solid content. Thus, assuming low χ_0 values, the FBD moisture content mass balance is :

$$\frac{d\chi_p}{dt} = a_1 \dot{V}_{0,sp}(\chi_0 - \gamma(T_p)\psi(\chi_p)) \tag{7}$$

where a_1 is an empirical parameter that represents the gas-particle mass transfer ratio per unit volume and $\dot{V}_{0,sp}$ is the volumetric flow setpoint.

3.2 Energy balance

Drying processes involve vaporization of the binding solution, here water. Since the latent heat of vaporization often exceeds the vapor heat, the latter is neglected. Thermodynamics properties, here densities and specific heat capacities, are considered constant. Heat losses are also neglected. Thus, the particle energy balance is :

$$\frac{dT_p}{dt} = b_1 \dot{V}_{0,sp}(\chi_0 - \gamma(T_p)\psi(\chi_p)) + b_2 \dot{V}_{0,sp}(T_0 - T_p) \tag{8}$$

where b_1 and b_2 are empirical coefficients that both represent gas-particle ratios for enthalpies and heat transfer.

3.3 Inlet blower and heater

The inlet gas moisture content χ_0 is assumed to be constant. On the pilot FBD, inlet gas temperature and flow rate are controlled by proportional-integral-derivative controllers (PIDs). Since the closed-loop time response between the volumetric flow setpoint $\dot{V}_{0,sp}$ ($\mathrm{m^3\,s^{-1}}$) and the corresponding value $\dot{V}_0$ ($\mathrm{m^3\,s^{-1}}$) is short, it is simply assumed that $\dot{V}_0 = \dot{V}_{0,sp}$.

The model between inlet temperature setpoint $T_{0,sp}$ (°C) and value T_0 (°C) is :

$$\frac{dT_0}{dt} = \frac{T_{0,sp} - T_0}{\tau_T} \tag{9}$$

where τ_T is the inlet temperature time constant.

A grey-box identification algorithm is used to calibrate the model with datasets coming from FBD batch experimentations. The resulting parameters are given in Table 1.

3.4 State-space representation

Equations (5) to (9) describe the single phase model, the states being

$$\mathbf{x}(t) = [T_0(t)\ \ \chi_p(t)\ \ T_p(t)]^T \tag{10}$$

This system is dicretized by a fourth order Runge-Kutta (RK4) method with a sampling time of 45s :

$$\mathbf{x}(k+1) = \mathbf{f}\Big(\mathbf{x}(k), \mathbf{u}(k)\Big) \tag{11a}$$

$$\mathbf{y}_T(k) = \mathbf{C}_T\mathbf{x}(k) = \begin{bmatrix} 1 & 0 & 0 \\ 0 & 0 & 1 \end{bmatrix} \mathbf{x}(k) \tag{11b}$$

$$y_\chi(k) = \mathbf{C}_\chi\mathbf{x}(k) = [0\ \ 1\ \ 0]\,\mathbf{x}(k) \tag{11c}$$

where $\mathbf{f}(\bullet)$ model state update function. The model outputs are $\mathbf{y}_T(k)$ and $y\chi(k)$. They are split into two equations to simplify the observer equations when the moisture content measurement is not available.

Table 1. Single phase batch fluidized dryer model parameter

parameter	units	value
a_1	$\mathrm{m^{-3}}$	9.32E-05
b_1	$\mathrm{°C\,m^{-3}}$	4.69E-02
b_2	$\mathrm{m^{-3}}$	2.61E-05
χ_{pc}		2.80E-02
χ_0		1.50E-03
α		4.90E-03
β	$\mathrm{°C^{-1}}$	5.70E-02
ν		3.04
τ_T	s	86.7

4. OBSERVER-BASED SOFT SENSORS

The observer-based soft sensors are derived from the MHE optimization-based algorithm. State estimation requires measurements :

$$\mathbf{y}_{T,m}(k) = [T_{0,m}(k)\ \ T_{p,m}(k)]^T \tag{12a}$$

$$y_{\chi,m}(k) = \frac{w_{p,m}(k)}{100 - w_{p,m}(k)} \tag{12b}$$

where $T_{0,m}$ (°C) and $T_{p,m}$ (°C) are the inlet gas and particle temperature measurements, respectively. $w_{p,m}$ (%) is the measurement of the wet basis moisture content in the particles. The model input vector $\mathbf{u}$ are the PID controller setpoints :

$$\mathbf{u} = \left[T_{0,sp}\ \ \dot{V}_{0,sp}\right]^T \tag{13}$$

4.1 Open-loop observers

The first two soft sensors are open-loop estimators, i.e. they are the simulation of the two-phase and single phase models fed by the input vector $\mathbf{u}$ and without measurement feedback. State estimation is performed by recursively solving the discrete state-space representation presented in Gagnon et al. (2020a) or the equations (11a) to (11c) for both models respectively with the same initial conditions described in the next section.

4.2 Moving horizon estimator

The proposed design makes use of the modifications introduced by Gagnon et al. (2017), i.e. the MHE in the predictor form, and a simplified arrival cost. The notation $\hat{\mathbf{x}}_j(i)$ refers to the estimated state vector at the discrete time i estimated at the discrete time j.

The optimization problem is :

$$\min_{\hat{\mathbf{x}}_k(k-N),\hat{\mathbf{W}}_k} \Phi_k + \hat{\mathbf{Z}}_k^T \bar{\mathbf{M}} \hat{\mathbf{Z}}_k \tag{14}$$

in which the first term of the cost function Φ_k is :

$$\begin{aligned}\Phi_k = &\Big(\hat{\mathbf{x}}_k(k-N) - \bar{\mathbf{x}}_k\Big)^T \mathbf{P}^{-1} \Big(\hat{\mathbf{x}}_k(k-N) - \bar{\mathbf{x}}_k\Big) \\ &+ \hat{\mathbf{W}}_k^T \bar{\mathbf{Q}}^{-1} \hat{\mathbf{W}}_k + \hat{\mathbf{V}}_k^T \bar{\mathbf{R}}^{-1} \hat{\mathbf{V}}_k\end{aligned} \tag{15}$$

where N is the dimension of the observation window and subject to the disturbed model :

$$\hat{\mathbf{x}}_k(k+1) = \mathbf{f}\Big(\hat{\mathbf{x}}_k(k),\ \mathbf{u}(k)\Big) + \hat{\mathbf{w}}(k) \tag{16a}$$
$$\mathbf{y}_T(k) = \mathbf{C}_T \mathbf{x}(k) + \hat{\mathbf{v}}(k) \tag{16b}$$
$$y_\chi(k) = \mathbf{C}_\chi \mathbf{x}(k) + \hat{z}(k) \tag{16c}$$

and constrained by :

$$\hat{\mathbf{x}}_{\min} < \hat{\mathbf{x}}_k(k-i) < \hat{\mathbf{x}}_{\max}\ \forall\ i\ \in\ [-1 \dots \min\{k, N\}] \tag{17}$$

In the disturbed model equations (16a) and (16b), $\mathbf{w}$, $\mathbf{v}$ are the process noise vector and measurement noise vector. They are considered white Gaussian noise signals with covariance matrices $\mathbf{Q}$ and $\mathbf{R}$ respectively. In equation (16c), z is the moisture content measurement noise and it is considered a white Gaussian noise signal with variance $1/M_i$. Weighs in (14) are diagonal matrices such as :

$$\bar{\mathbf{Q}} = \text{diag}\Big(\mathbf{Q}, \mathbf{Q}, \dots, \mathbf{Q}\Big)_{[3(N+1)\times 3(N+1)]} \tag{18a}$$
$$\bar{\mathbf{R}} = \text{diag}\Big(\mathbf{R}, \mathbf{R}, \dots \mathbf{R}\Big)_{[2(N+1)\times 2(N+1)]} \tag{18b}$$
$$\bar{\mathbf{M}} = \text{diag}\Big(M_{-N}, M_{-N+1}, \dots, M_0\Big)_{[(N+1)\times(N+1)]} \tag{18c}$$
$$\mathbf{P} = \text{Cov}\Big(\mathbf{x}(k-N), \hat{\mathbf{x}}_k(k-N)\Big)_{[3\times 3]} \tag{18d}$$

In the cost function in (14), the estimated process and measurement noises over the observation window are :

$$\hat{\mathbf{W}}_k = \begin{bmatrix} \hat{\mathbf{w}}(k-N+0) \\ \hat{\mathbf{w}}(k-N+1) \\ \vdots \\ \hat{\mathbf{w}}(k) \end{bmatrix} \tag{19a}$$

$$\hat{\mathbf{V}}_k = \begin{bmatrix} \mathbf{y}_{T,m}(k-N+0) - \mathbf{C}_T \hat{\mathbf{x}}_k(k-N+0) \\ \mathbf{y}_{T,m}(k-N+1) - \mathbf{C}_T \hat{\mathbf{x}}_k(k-N+1) \\ \vdots \\ \mathbf{y}_{T,m}(k) - \mathbf{C}_T \hat{\mathbf{x}}_k(k) \end{bmatrix} \tag{19b}$$

$$\hat{\mathbf{Z}}_k = \begin{bmatrix} y_{\chi,m}(k-N+0) - \mathbf{C}_\chi \hat{\mathbf{x}}_k(k-N+0) \\ y_{\chi,m}(k-N+1) - \mathbf{C}_\chi \hat{\mathbf{x}}_k(k-N+1) \\ \vdots \\ y_{\chi,m}(k) - \mathbf{C}_\chi \hat{\mathbf{x}}_k(k) \end{bmatrix} \tag{19c}$$

They are obtained by recursively solving the disturbed model equation :

$$\hat{\mathbf{x}}_k(k-i+1) = \mathbf{f}\Big(\hat{\mathbf{x}}_k(k-i),\ \mathbf{u}(k-i)\Big) + \hat{\mathbf{w}}(k-i) \tag{20}$$

When the optimal arguments, $\hat{\mathbf{x}}_k(k-N)$ and $\hat{\mathbf{W}}_k$, are computed, the state estimation at the next discrete time $\hat{\mathbf{x}}_k(k+1)$ is obtained by recursively applying equation (20) down to $i = 0$. Equation (14) is solved with MATLAB function `fmincon` using a combination of sequential quadratic programming method and central finite difference calculations. Discrete time is incremented and this estimated state is used as the observer output. The MHE optimisation problem is initialized with $\bar{\mathbf{x}}_\mathbf{k}$ which is :

$$\bar{\mathbf{x}}_k = \begin{cases} \bar{\mathbf{x}}_0 & \text{if } k \le N \\ \hat{\mathbf{x}}_{k-N-1}(k-N) & \text{if } k > N \end{cases} \tag{21}$$

where $\bar{\mathbf{x}}_0 = \Big[T_{0,m}(0)\ \ \frac{w_{p,m}(0)}{100-w_{p,m}(0)}\ \ T_{p,m}(0)\Big]^T$.

4.3 Closed-loop observer 1 : no moisture content measurement

The third soft sensor is the closed-loop observer 1 (CLO1) in which no moisture content measurement is taken into account. Thus, the weights in equation (18c) become :

$$M_i = 0\ \forall\ i \tag{22}$$

4.4 Closed-loop observer 2 : delayed moisture content measurement

State estimation, provided by the MHE, is performed here for N discrete time in the past. Thus, a delayed at-line moisture content measurement can be inserted into the observation window at the time it was taken leading to the closed-loop observer 2 (CLO2).

$w_{p,m}(l)$ is an at-line loss on drying (LOD) measurement, taken at time l but only becoming available at the time k because of the analysis time. Thus, at present time k, the measurement can be inserted in equation (19c) with the delay being fixed at $d = k - l$:

$$y_{\chi,m}(k+i) = \begin{cases} \frac{w_{p,m}(l)}{100-w_{p,m}(l)} & i = -d \\ 0 & \text{otherwise} \end{cases} \tag{23}$$

The weights are adjusted accordingly in equation (18c) :

$$M_i = \begin{cases} m & i = -d \\ 0 & \text{otherwise} \end{cases} \tag{24}$$

At the next sampling time, the measurement value and the weight are shifted :

$$y_{\chi,m}(k+i) = \begin{cases} \frac{w_{p,m}(l)}{100-w_{p,m}(l)} & i = -d-1 \\ 0 & \text{otherwise} \end{cases} \tag{25}$$

$$M_i = \begin{cases} m & i = -d-1 \\ 0 & \text{otherwise} \end{cases} \tag{26}$$

Shifting is repeated at the next sampling periods until the values exit the time windows.

4.5 Closed-loop observer 3 : delayed moisture content and virtual measurements

A methodology is proposed to propagate the at-line LOD measurement leading to closed-loop observer 3 (CLO3). The idea consists in calculating, at the time the LOD measurement becomes available, virtual moisture content measurements $\tilde{y}_\chi(-d+1), \ldots, \tilde{y}_\chi(0)$ to fill the lower part of the observation window. This is achieved by recursively solving equations (11a) and (11c) with the initial condition $\left[T_{0,m}(l) \ \frac{w_{p,m}(l)}{100-w_{p,m}(l)} \ T_{p,m}(l)\right]^T$. Thus, at present time k, moisture content measurement in equation (19c) become :

$$y_{\chi,m}(k+i) = \begin{cases} \frac{w_{p,m}(l)}{100-w_{p,m}(l)} & i = -d \\ \tilde{y}_\chi(i) & i \in [-d+1 \ldots 0] \\ 0 & \text{otherwise} \end{cases} \quad (27)$$

and, in equation (18c), the weights become :

$$M_i = \begin{cases} m & i \in [-d \ldots 0] \\ 0 & \text{otherwise} \end{cases} \quad (28)$$

At the next sampling time a new virtual measurement is obtained by pursuing one more step of the previous calculations with (11a) and (11c). This new value is inserted and the previous ones are shifted:

$$y_{\chi,m}(k+i) = \begin{cases} \frac{w_{p,m}(l)}{100-w_{p,m}(l)} & i = -d-1 \\ \tilde{y}_\chi(i) & i \in [-d \ldots 0] \\ 0 & \text{otherwise} \end{cases} \quad (29)$$

$$M_i = \begin{cases} m & i \in [-d-1 \ldots 0] \\ 0 & \text{otherwise} \end{cases} \quad (30)$$

The same process is repeated at each sampling period. If a new at-line moisture content measurement becomes available, the new value is calculated and inserted in the appropriate positions in (18c) and (19c), while keeping previous values, if any, elsewhere in the vector/matrix.

4.6 Closed-loop observers parameters

CLO2 offers a way to simply handle an at-line moisture content measurement. However, the delay associated with the analysis time implies that this value is inserted near the end of the observation window resulting in little to no effect on the estimation accuracy. Since CLO1 and CLO2 performances are almost identical, CLO2 will not be further analyzed. For both CLO1 and CLO3, the selected parameters are :

- $\Delta t = 45$s
- $N = 12$
- $\hat{\mathbf{x}}_{\min} = [40 \ 0 \ 20]^T$
- $\hat{\mathbf{x}}_{\max} = [95 \ 20 \ 70]^T$
- $m = 1/1.338$
- $\mathbf{P} = \text{diag}(0.01, 5, 3)$
- $\mathbf{Q} = \text{diag}(0.1, 10, 30)$
- $\mathbf{R} = \text{diag}(2.544, 0.487)$

$\mathbf{R}$ and m were selected from the instrument noise magnitude. $\mathbf{Q}$ and $\mathbf{P}$ were selected by trial and error.

State estimation constraints were selected at 0% for particle moisture content on dry basis, 40 and 95°C on the inlet gas temperature (operating limits), and 20 and 70°C on the particle temperature (minimum and maximum values observed in practice).

5. RESULTS

Open-loop operation of the FBD is performed with experimental setup described in section 2. The sampling period of the FBD sensors is 45 s. The open-loop observers (here two-phase and single phase models) are simulated with the algorithm given in section 4.1 and theses simulations are performed with the same sampling time as the FBD sensors. The closed-loop observers (here CLO1 and CLO3) are simulated with the algorithm given in sections 4.2, 4.3 and 4.5. In-line measurement provide feedback for the inlet gas and particle temperatures every 45 s. For CLO3, a single moisture content inline measurement is provided after 2 minutes of operation.

The difference between the estimated states and measurements (inlet gas temperature, humidity from NIR probe and particle temperature) gives the estimation error. The performance benchmarks are based on the root mean square error (RMSE) of estimation. Table 2 and Figure 1 provide the results for between all soft sensors for three batches.

For particle temperature, these results show that both closed-loop MHE have higher estimation accuracy than open-loop observers. This difference is explained by the measurement feedback provided to the algorithm. Particle temperature measurement feedback alone can also result in better moisture content estimation as it is shown in B3 where high particle temperature estimation error was observed for the single phase open-loop observer. Thus, the CLO1 estimation accuracy is better than the single phase model for both particle moisture content and temperature even if no moisture content measurement feedback is provided.

In the event of a large moisture content estimation error, the results show that providing a single moisture content measurement can largely improve estimation accuracy as it is shown by CLO3 in B1 and B3. In the other case, moisture content estimation is not impaired as depicted for B2. These results show that CLO3 is able to reproduce

Table 2. RMSE values of the four observers presented in this article

		RMSE		
case	batch	T_0 (°C)	w_p (%)	T_p (°C)
Two-phase	B1	3.319	1.549	3.875
	B2	1.812	1.228	4.735
	B3	2.896	0.486	4.538
Single phase	B1	2.322	3.705	9.373
	B2	2.801	0.514	1.377
	B3	2.899	1.034	8.073
CLO1	B1	2.796	3.614	2.141
	B2	1.791	0.440	0.955
	B3	2.698	0.692	1.396
CLO3	B1	2.815	2.180	2.103
	B2	1.610	0.454	1.067
	B3	2.465	0.468	1.107

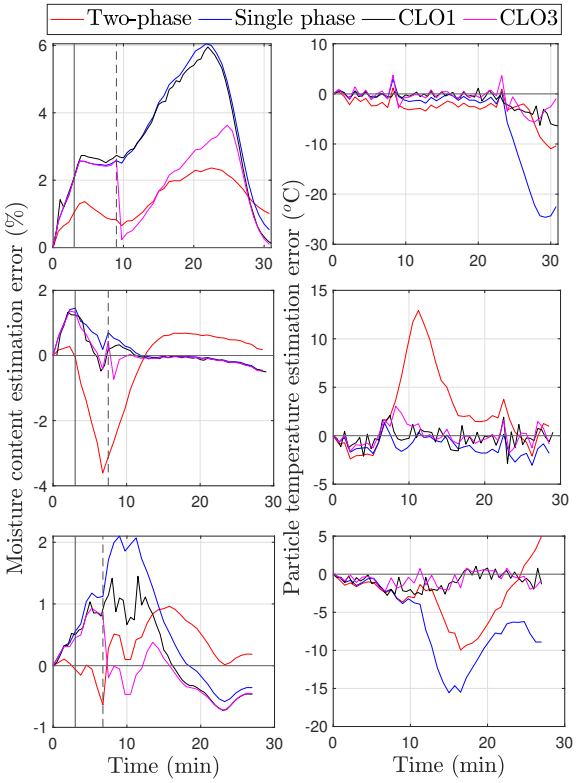

Fig. 1. Estimation error with pilot FBD data: batches B1 (top), B2 (middle) and B3 (bottom). Offline measurement is being taken and made available at the solid vertical line and dash vertical line, respectively.

data as accurately or better than the full-blown two-phase phenomenological model.

6. CONCLUSION

This work proposes five moisture content soft sensors: two phenomenological models, i.e. one based on a detailed two-phase description, and the other one, on a single phase simplified one, and three MHE designs using the latter single phase model. Results show that the simplifying assumptions made for the single-phase model does not curb the performance, and closed-loop MHEs can accurately reproduce data taken from a pilot scale FBD. Feedback using both delayed moisture content, and virtual measurements leads to estimations similar to that from the complex phenomenological model, but with obviously lower computational effort and higher robustness. This makes the corresponding MHE adequate to pair with a real-time optimization control of the FBD. Future developments will tackle this issue.

ACKNOWLEDGEMENTS

The authors would like to thank the National Sciences and Engineering Council of Canada (NSERC), Pfizer Canada and the Fonds de recherche du Québec : Nature et technologies (FRQNT) for funding this research.

REFERENCES

Gagnon, F., Bouchard, J., Desbiens, A., and Poulin, E. (2020a). Development and validation of a batch fluidized bed dryer model for pharmaceutical particles. *Drying Technology*, 1–24. doi:10.1080/07373937.2019.1701005.

Gagnon, F., Desbiens, A., Poulin, E., and Bouchard, J. (2020b). Simplified modelling of a batch fluidized bed dryer for control purposes. Submitted to 59nd on Decision and Control, Jeju Island, Korea.

Gagnon, F., Desbiens, A., Poulin, E., Lapointe-Garant, P.P., and Simard, J.S. (2017). Nonlinear model predictive control of a batch fluidized bed dryer for pharmaceutical particles. *Control Engineering Practice*, 64, 88–101.

Haseltine, E. and Rawlings, J. (2005). Critical evaluation of extended kalman filtering and moving–horizon estimation. *Industrial & Engineering Chemistry Research*, 44(8), 2451–2460.

Jensen, S., Da Cruz Meleiro, L.A., and Zanoelo, É.F. (2011). Soft sensor model design for control of a virtual conveyor-belt dryer of mate leaves (ilex paraguariensis). *Biosystems Engineering*, 108(1), 75–85.

Lauri Pla, D., Kamyar, R., Hashemian, N., Mehdizadeh, H., and Moshgbar, M. (2018). Moisture soft sensor for batch fluid bed dryers: A practical approach. *Powder Technology*, 326, 69–77.

Li, M. and Duncan, S. (2008). Model–based nonlinear control of batch fluidized bed dryers. *Particle & Particle Systems Characterization*, 25(4), 345–359.

Obrégon, L., Quiones, L., and Veláquez, C. (2013). Model predictive control of a fluidized bed dryer with an inline nir as moisture sensor. *Control Engineering Practice*, 21, 509–517.

Rao, C. and Rawlings, J. (2002). Constrained process monitoring: Moving–horizon approach. *AIChE J.*, 48(1), 97–109.

Roggo, Y., Chalus, P., Maurer, L., Lema-Martinez, C., Edmond, A., and Jent, N. (2007). A review of near infrared spectroscopy and chemometrics in pharmaceutical technologies. *Journal of Pharmaceutical and Biomedical Analysis*, 44, 683–700.

Tok, A.T., Goh, X., Ng, W.K., and Tan, R.B. (2008). Monitoring granulation rate processes using three pat tools in a pilot-scale fluidized bed. *AAPS PharmSciTech*, 9(4), 1083–1091.

Valencia, F., López, J.D., Marquez, A., and Espinosa, J. (2011). Moving horizon estimator for measurement delay compensation in model predictive control schemes. In *2011 50th IEEE Conference on Decision and Control and European Control Conference*, 6678–6683.

Vieira, G.N.A., Olazar, M., Freire, J.T., and Freire, F.B. (2019). Real-time monitoring of milk powder moisture content during drying in a spouted bed dryer using a hybrid neural soft sensor. *Drying Technology*, 37(9), 1184–1190.

Zhang, W., Cheng, X., Hu, Y., and Yan, Y. (2019). Online prediction of biomass moisture content in a fluidized bed dryer using electrostatic sensor arrays and the random forest method. *Fuel*, 239, 437–445.